Predicting Thermal Conductivity of Amorphous Polymers with Temperature Variations: An Empirical Model

***Dr. Gajendra Gupta**

Abstract

Thermal conductivity of polymers has been extensively researched, both theoretically and practically, but more precise models are required. Existing models do not adequately account for polymeric thermal conductivity's plateau-like change at temperatures around 10 K. This paper presents an empirical model for predicting temperature-dependent thermal conduction of amorphous polymers. The model depends on kinetic theory and takes into consideration three distinct types of vibrational modes in polymers. It was constructed using classical formulas, previous simulation results, and experimental data. Only fundamental material variables such as density, monomers molecular weight, and sound speed are used as input parameters. The model generates estimates for the sites of transitions between various kinds of vibrational modes, an upper limit for thermal conductivity, and dependent on temperature thermal conductivity that are consistent with experimental results.

Keywords: thermal conductivity, amorphous polymers, vibrational modes, temperature-dependent models, kinetic theory, empirical model

Introduction

Organic thermoelectrics, with low thermal conductivity (<1 $Wm^{-1}K^{-1}$), are studied to optimize the thermoelectric power factor. Accurate predictive models are essential, as existing ones fail to capture vibrational physics across temperature ranges.

Crystalline vs. Amorphous Materials

Figure 1 contrasts thermal conductivity in crystalline (e.g., Ag, Si) and amorphous materials (e.g., polymers like PS, PTFE). Crystalline materials follow phonon transport theories, while amorphous materials show temperature-dependent behaviors involving propagating (propagons) and non-propagating (diffusons, locons) vibrational modes.

Empirical Model for Polymers

We propose a model predicting polymer thermal conductivity from 1–300 K using:

1. Sound velocity,
2. Monomer molecular mass,
3. Gravimetric density.

The model, with $R^2 > 75\%$, predicts conductivity trends, vibrational mode transitions, and upper limits.

Vibrations in Amorphous Materials

Amorphous materials lack regular atomic order, leading to distinct vibrational modes. Thermal transport depends on propagons, diffusons, and locons, with mode transitions defined by the Ioffe-Regel crossover and mobility edge. This study simulates these modes in polymers, linking them to temperature-dependent thermal conductivity, providing crucial insights for thermoelectric applications.

Earlier Models of Thermal Conductivity

The Einstein model, limited by its single vibrational frequency assumption, poorly aligns with experimental data. The Cahill-Pohl *k*-min model improves predictions using Debye theory, achieving order-of-magnitude accuracy at ambient temperatures but underpredicting low-temperature thermal conductivity (Figure 4, polystyrene).

Advanced simulations, like Green-Kubo formalism and lattice dynamics, help analyze vibrational domains—propagons, diffusons, and locons. While scaling thermal conductivity using monomer molecular weight offers promise, challenges in parameter definitions and plateau predictions necessitate further polymer-specific research.

Using kinetic theory

Using kinetic theory, we developed an empirical model for thermal conductivity, k, defined as a function of vibrational diffusivity D and volumetric heat capacity c:

$$k = \frac{1}{3} c D \tag{1}$$

The model accounts for all vibrational modes via specific heat and diffusivity as functions of vibrational frequency. The equation integrates over the vibrational frequency spectrum:

$$k = \frac{1}{3} \int c(\omega) \, D(\omega) \, N(\omega) \, d\omega \tag{2}$$

where $N(\omega)$ (in [#-s]) is the density of states, signifying the quantity of vibrational modes in the frequency range between ω and $d\omega$ (in [rad·s^{-1}]). We divided the integral in the equation into three sections, which correspond to propagons (P), diffusons (D), and locons (L), in order to account for the many kinds of vibrations in polymers. Between their corresponding frequency limits, each kind of vibration is integrated:

- (i) ω=0 rad·s^{-1} and the Ioffe-Regel cross-over (ω_P) are for propagons,
- (ii) the Ioffe-Regel crossover and mobility edge (ω_D) are for diffusions, and
- (iii) the mobility edge and infinity are for locons.

Cutoff frequency for the diffusons and propagons are provided by the mobility edge and the Ioffe-Regel crossover, respectively. While the Ioffe-Regel crossover usually occurs over a frequency range, for simplicity we use a sharp cutoff between diffusons and propagons in our model. According to the connection $k_B T$ (i=P,D,L), this cutoff frequency can also be represented as an identical cutoff temperature, enabling us to use the terms cutoff frequency and cutoff temperature interchangeably. Additionally, we use a dimensionless cutoff, $x_i = {\hbar\omega_i}/{k_B T} = {T_i}/{T}$, as a handy way to change variables.

Consequently, the following is an expression for the total thermal conductivity,

k ⍰ k_P ⍰ k_D ⍰ k_L =

$$= \frac{1}{3}\sum_{i=P,D,L}\int_{\omega_{i-1}}^{\omega_i} c_i(\omega) D_i(\omega) N_i(\omega)\, d\omega \qquad (3)$$

Particular Heat

The volumetric specific heat is determined by treating each vibrational mode as a one-dimensional oscillator, summed over all directions (Eq. 4). This approach models propagons well, as they resemble phonon-like vibrations. The equation's accuracy is supported by experimental data for materials like a-SiO_2 and a-Si, and is also applied to non-propagating modes.

The diffusivity of

$$c = 3nk_B \frac{x^2 e^x}{\left(e^x - 1\right)^2},\ x = \frac{\hbar\omega}{k_B T} \qquad (4)$$

The vibrational diffusivity, D(ω), is proportional to the vibrational frequency and propagation speed (vs), estimated as the speed of sound. This formula, which describes both diffusons and locons, is preferred over the more complex Allen and Feldman model, typically used for propagating modes. The diffusivity follows a ω^{-2} dependence for diffusons, as shown in Eq. (5):

$$D\ \square\omega\square\ \square\ v\ {}^{2}\omega^{\square\,\beta}\mathrm{i} \qquad (5)$$

In this equation, the type of vibration mode (propagons, diffusons, or locons) is indicated by the subscript i. The exponent βi for propagating modes in amorphous materials spans from 2 to 4, according to molecular dynamics (MD) simulations; however, it is closer to 2 for non-propagating modes. For this reason, we keep βi as a fitting parameter in our model.

State Density

Under the Debye approximation, we use the following formula for the number of states in three dimensions: The formula

$$N(\omega) = \frac{3V\omega^2}{2\Pi^2 v_s^3} \qquad (6)$$

where the volume of a unit cell is denoted by V (in m 3). In contrast to crystalline materials, it is more difficult to define a unit cell in a polymer. Nonetheless, we may roughly estimate that the number density nn (in m−3−3) is inversely proportional to the volume of a unit cell. As a result, the density of states can be stated proportionally as

$$N(\omega) = \frac{3V\omega^2}{2\Pi^2 v_s^3} \qquad (7)$$

The Study's Consideration of Polymers

Figure 2 displays the experimental results for temperature-dependent thermal conductivity in the studied polymers. The modal properties are based on number density and sound speed, with the speed of sound calculated using the average of longitudinal and transverse modes. When experimental data is unavailable, Eq. (8) uses shear (G) and bulk (K) moduli. The number density, (*i.e.*, $n = \rho N_A/M$, where N_A is the Avogadro constant.

The properties that were used to develop our model are compiled in Table 1, including the number density (n), gravimetric density (ρ), molecular weight of the monomer unit (M), speed of sound (v_s), and individual the references for the experimental information for dependent on temperature thermal conductivity.

$$v_{s,\text{trans}} = \sqrt{\frac{G}{\rho}};\quad v_{s,\text{long}} = \sqrt{\frac{4G+3K}{3\rho}} \qquad (8)$$

Model-I

Eq. (9), which is a dependent on temperature expression for the thermal conductivity, is obtained by substituting Eqs. (4), (5), and (7) into Eq. (3). By adding a proportional constant, f_i, which depends on the kind of vibrational mode, the proportionality can be stated as an equality. In total, there are eight unknowns in Eq. (9):

(i) three proportionality coefficients, f_i,

(ii) two devoid of dimensions cutoffs (the mobility edge and the Ioffe-Regel crossover), x_i, and

(iii) three exponents β_i for each of the three vibrational mode types.

$$k(T) = \frac{k_B}{v_s} \sum_{i=P,D,L} \left(\frac{k_B T}{\hbar} \right)^{3-\beta_i} \int_{x_{i-1}}^{x_i} f_i \frac{x^{4-\beta_i} e^x}{\left(e^x - 1\right)^2} dx \qquad (9)$$

The non-dimensional counterparts of the previously stated frequency cutoffs are the limits of the integral.

EXPERIMENTAL

Thermal conductivity of five polymers—PMMA, PS, PTFE, PVC, and PVA—was measured from 10 K to 300 K. The samples included a 1 mm thick PTFE substrate and ~1 µm thick films of PMMA, PS, PVC, and PVA on a Si substrate. Films were prepared via drop-casting (PVA, PS) or spin-coating (others).

Thermal conductivity was measured using the 3-omega (3ω) method, with the slope method applied to the PTFE substrate and the differential method to the thin films. Measurements were conducted in a closed-loop liquid helium cryostat for precise temperature control.

OUTCOMES AND TALK

Model-I Results

The empirical model (Eq. 9) was fitted to thermal conductivity data for 12 polymers, yielding a coefficient of determination $R^2 > 0.95$. This high accuracy reflects the model's ability to capture the data despite eight fitting parameters.

Locons' Contribution

Thermal conductivity curves (k-T) for most polymers show a plateau below 10 K, marking the transition between propagons and diffusons. A similar diffuson-locon transition is rarely observed due to the glass transition near ambient temperature, resulting in negligible locon contributions. This aligns with MD simulations of a-Si and a-SiO_2, confirming that propagons and diffusons dominate heat transport. The model is thus simplified to six fitting parameters, focusing on these two modes.

The Exponent, β

Quartile analysis of the exponents β_p (propagons) and βi (diffusons) reveals:

- βi is consistently close to 1 for all polymers (0.95 ≤ βi ≤ 1.05), allowing βi=1 as a fixed value (R^2>0.95).
- β_P varies slightly (1.1 ≤ β_P ≤ 1.31), with β_P=1.2 providing a reliable prediction (R^2>0.90).

At low temperatures (<1 K), the model predicts a $T^{1.8}$ dependence for thermal conductivity, consistent with observations for disordered crystals and amorphous inorganic materials below the first plateau.

Model II

We may reduce the expression in Eq. (9) to the following by using the insights from the prior fitting procedure:

$$k(T) = f_P \frac{k_B}{v_s}\left(\frac{k_B T}{h}\right)^{1.8}\int_0^{x_P}\frac{x^{2.8}e^x}{\left(e^x-1\right)^2}dx + f_D \frac{k_B}{v_s}\left(\frac{k_B T}{h}\right)^{2}\int_{x_P}^{x_D}\frac{x^{3}e^x}{\left(e^x-1\right)^2}dx \tag{10}$$

A key outcome is the simplified model considering only diffusons and propagons with fixed diffusivity exponents. Propagon and diffuson contributions are represented by the two terms in Eq. (10), with four fitting parameters: f_P and f_D, as well as the dimensionless cutoffs x_P and x_D for diffusons and propagons.

We carried out a fitting procedure for the twelve polymers as before. (The Supplemental Information provides a detailed presentation of the fitting results, emphasizing the connections among the various factors.) An inverse power-law relationship exists between the coefficients f_P and f_D and the cutoff temperatures T_P and T_D, respectively. The coefficients f_P and f_D for diffusons and propagons likewise show a similar relationship.

The link between the coefficient of determination (R^2), the best-fit equations, and the fitting parameters for the inverse power-law fits is displayed in Figure 6(a-c). The best-fit inverse power-law equations are compiled in Eqs. (11–13). R2 values for the three equation fits are 0.81, 0.78, and 0.90, in that order. In these inverse power-law fits, f_P is in $s^{-0}.^{2}$, f_D is dimensionless, and the cutoff temperatures, T_P and T_D, are in K.

$T_p = 53.94\ f_p^{-0.278}$ (11)

$T_D = 72.27\ f_D^{-0.283}$ (12)

$F_D = 25.09\ f_p^{-0.768}$ (13)

Relating T_D to fundamental properties

In order for our model to be complete, one of the four variables must be related to basic material properties like ρ, M, and v_s. Eq. (14), which denotes the maximum temperature attained from a single normal vibration, can be used to define a Debye temperature for crystalline materials. We apply the same definition to polymers, using the average of the longitudinal and transverse directions of the speed of sound for v_s and the monomer molecular weight for M.

Using this updated concept of a Debye temperature, we use an inverse power law fit with a R^2 of 0.84 (see Figure 7) to connect the diffuson cutoff temperature T_D to T_{Deb} (in [K]) and ρ (in [kg·m^{-3}]).

$$T = \frac{v_s h}{K_B} (6\pi^2 n)^{1/3} \qquad (14)$$

$$T_D = 1.465 \times 10^7 \left(p \sqrt{T_{Deb}}\right)^{-1.23} \qquad (15)$$

The interpretation of T_P (and ω_P)

The Ioffe-Regel crossover, which denotes the change from propagons to diffusons, is represented by the propagon cutoff frequency, ω_P. This frequency is estimated by our model to be between 0.6 and 1.7 THz. This crossover happens at a frequency where the mean-free-path (l_{mfp}) is roughly ten times the interatomic distance (a), according to earlier research. Based on the propagon cutoff the frequency, speed of sound, and number density, the order of magnitude of the ratio l_{mfp}/a for the polymers taken into consideration in this work may be ascertained (Eq. (16)). According to our model, this ratio is roughly 10.

$$\frac{l_{mfp}}{a} \approx \frac{2\pi v_s n^{1/3}}{\omega_p} \qquad (16)$$

Understanding f_P and f_D

$$k_{\mathrm{P}}(T) = 1.85\frac{{f_{\mathrm{P}}}^{0.5}}{v_{\mathrm{s}}}\left[\frac{1}{{x_{\mathrm{P}}}^{1.8}}\int_0^{x_{\mathrm{P}}}\frac{x^{2.8}e^x}{\left(e^x-1\right)^2}dx\right]$$
$$k_{\mathrm{D}}(T) = 1226\frac{{f_{\mathrm{D}}}^{0.43}}{v_{\mathrm{s}}}\left[\frac{1}{{x_{\mathrm{D}}}^{2}}\int_{x_{\mathrm{P}}}^{x_{\mathrm{D}}}\frac{x^{3}e^x}{\left(e^x-1\right)^2}dx\right]$$

(17)

Equation (17) shows how the propagon and diffuson contributions to thermal conductivity at a given temperature are expressed using the $f-T$ relations from Eqs. (11) and (12). The temperature-dependent variables in this equation are the dimensionless cutoffs, x_P and x_D. Our model suggests that the slope of the k−T curve will be 1.8 when temperatures are much lower than the propagon cutoff ($T \ll T_P$). In fully amorphous polymers, the contributions for diffusons and propagons reach maximum values of 0.5 and 0.56, respectively. These upper limits for k_P and k_D are governed by f_P, f_D, and v_s. The upper limit to the thermal conductivity can be expressed in terms of a single fitting parameter, as seen in Eq. (18), by replacing the terms in the brackets in Eq. (17) with the maximum values and adding the relationship between f_P and f_D from Eq. (12).

(18)

$$\begin{aligned} k_{\mathrm{max}} &= \frac{1}{v_{\mathrm{s}}}\left(1.036\, f_{\mathrm{P}}^{0.5} + \frac{2483.3}{f_{\mathrm{P}}^{0.33}}\right) \\ &= \frac{1}{v_{\mathrm{s}}}\left(\frac{1.430\times10^{13}}{\left(\rho\sqrt{T_{\mathrm{Deb}}}\right)^{2.83}} + 5.27\times10^{-6}\left(\rho\sqrt{T_{\mathrm{Deb}}}\right)^{1.87}\right) \end{aligned}$$

This study establishes the upper thermal conductivity limit for bulk amorphous polymers using our empirical model. While diffusons typically dominate over propagons, adjusting a polymer's density and sound speed could shift this balance. For example, a polymer with half the gravimetric density of polystyrene could have a propagon contribution significantly higher than the diffuson contribution.

Comparing our model with experimental data and the high-temperature k_{min} model, we find less than 5% deviation at 300 K.

$$k_{\mathrm{min,high\ T}} \approx 0.40 k_{\mathrm{B}} n^{2/3}\left(v_{\mathrm{s,long}} + 2v_{\mathrm{s,trans}}\right)$$

(19)

At 300 K, our model's upper limit is within 30% of experimental values and outperforms the $k_{\min}$ model (see Table 2).

Prediction of Thermal Conductivity

The empirical model predicted thermal conductivity for 17 polymers (1–300 K), with R^2 values above 0.75, and over 0.95 for some. Predictions closely matched experimental data, including 3ω method results, accurately capturing the Ioffe-Regel crossover temperature, as shown in Figure 8.

In conclusion

We developed an empirical model to predict the thermal conductivity of polymers as a function of temperature. Unlike the $k$min model, which underperforms at lower temperatures, our model accounts for propagating vibrational modes and provides good estimates below 50 K. Based on kinetic theory, the model incorporates density of states, diffusivity, and modal specific heat. Numerical studies and classical expressions for density of states and specific heat were used, with fitting parameters linked to material properties like molecular weight, gravimetric density, and speed of sound. Our model is applicable to bulk amorphous polymers and predicts an upper thermal conductivity limit, typically within 30% of experimental values at 300 K. While it does not consider locons, which may lead to higher conductivities in certain polymers, the model accurately predicts the Ioffe-Regel crossover. For polymers not used in the fitting, the coefficient of determination (R^2) exceeds 0.75. Recent studies on room temperature polymer measurements show our model underpredicts thermal conductivity by less than 30%, likely due to unaccounted localized modes.

VISUAL ABSTRACT

Names of the authors

Shannon K. Yee and Sampath Kommandur

TITLE: An empirical model to forecast amorphous polymers' temperature-dependent thermal conductivity

Text message

An empirical model is developed to predict the temperature-dependent thermal conductivity of amorphous polymers using basic material properties like density, monomer molecular weight, and sound speed. The model aligns well with theoretical and experimental data, accurately forecasting thermal conductivity, mode transitions, and an upper conductivity limit.

GRAPHICAL ABSTRACT FIGURE

Figure 1:

An overview of the thermal conductivity of several solids, including metals (like silver), crystalline materials (like silicon and NaCl), amorphous solids (like a-SiO2), and polymers (like PS and PTFE). In contrast to the well-known tendencies in metals and crystalline materials (···), polymers and amorphous materials (—) exhibit monotonically rising thermal conductivity with temperature and experience a plateau-like transition at intermediate temperatures (about ~10 K). Every piece of information was sourced from references.

FIGURES AND TABLES

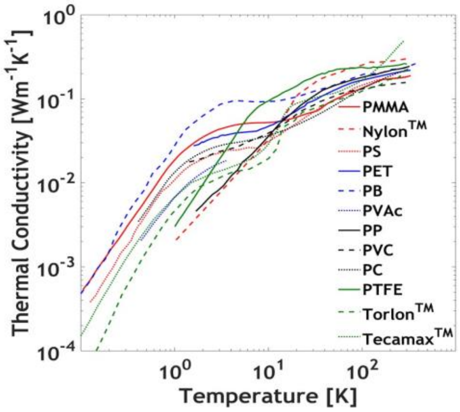

Figure 2:

Twelve distinct polymers' measured thermal conductivity as a function of temperature. It should be mentioned that because amorphous systems have a variety of vibrational modes, most polymers approach a plateau at higher temperatures (~300 K) and undergo a plateau-like transition at lower temperatures. For data sources, see Table 1.

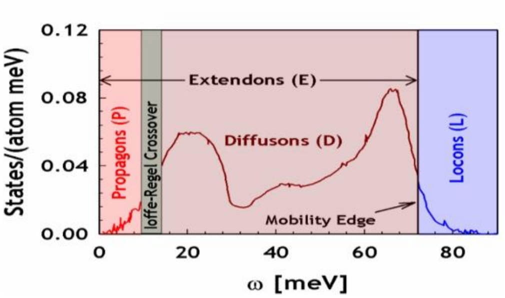

Figure 3:

Vibrational density of states for a-Si, as computed theoretically, showing the several sets of vibrational modes (propagons, diffusons, and locons).

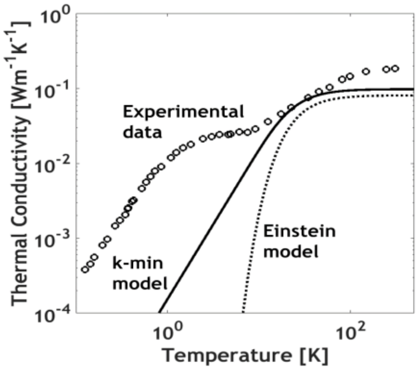

Figure 4:

Data on polystyrene's thermal conductivity and the matching predictions made by the k-min and Einstein models. For T > 10 K, the k-min model accurately predicts the thermal conductivity.

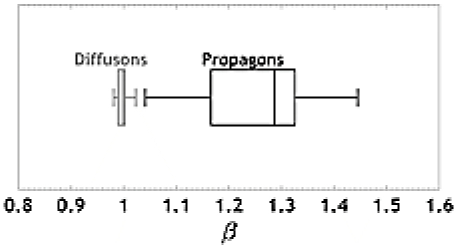

Figure 5:

By fitting the measured data to Model-I to produce quantile graphs showing the change in the exponents βP and βD. βD can be roughly represented as unity and exhibits a much narrower spread than βP. Since 70% of the polymers have βP between 1.1 and 1.3, βP is estimated to be about 1.2.

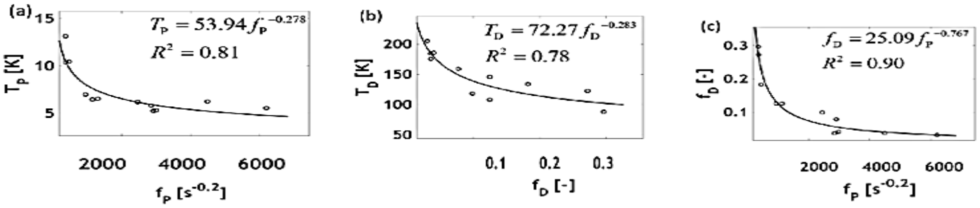

Figure 6:

Plotting the fitted parameters against each other reveals their inverse-power law relationship. Along with each plot's equations and R² values, the best fit is also displayed.

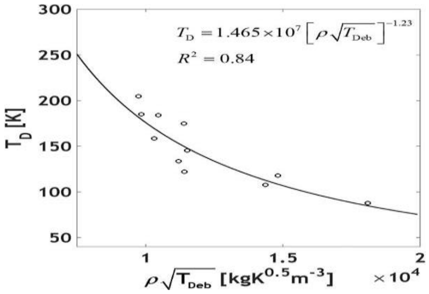

Figure 7:

The inverse power-law relationship is demonstrated by plotting the diffusion cutoff temperature (TD) against density and Debye temperature. The equation and R^2 value for the best least squares fit are also displayed.

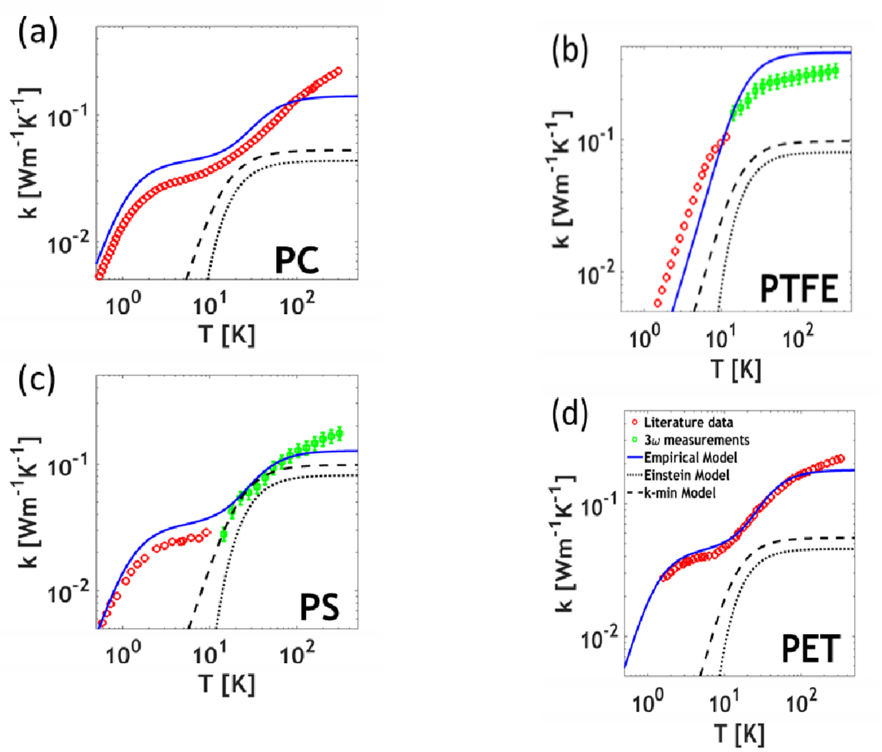

Figure 8:

Red hollow circles represent experimental thermal conductivity values found in the literature; green squares with error bars represent our 3-omega method data; and the solid blue line represents our empirical model predictions for four distinct polymers. PET, PTFE, PS, and PC are shown in Figures (a) through (d), respectively. The predictions of the k-min model (---) and Einstein model (···) are also displayed. Our empirical model's applicability is demonstrated by its consistently high R^2 value (>0.75). For references to experimental data from the literature, see Table 1.

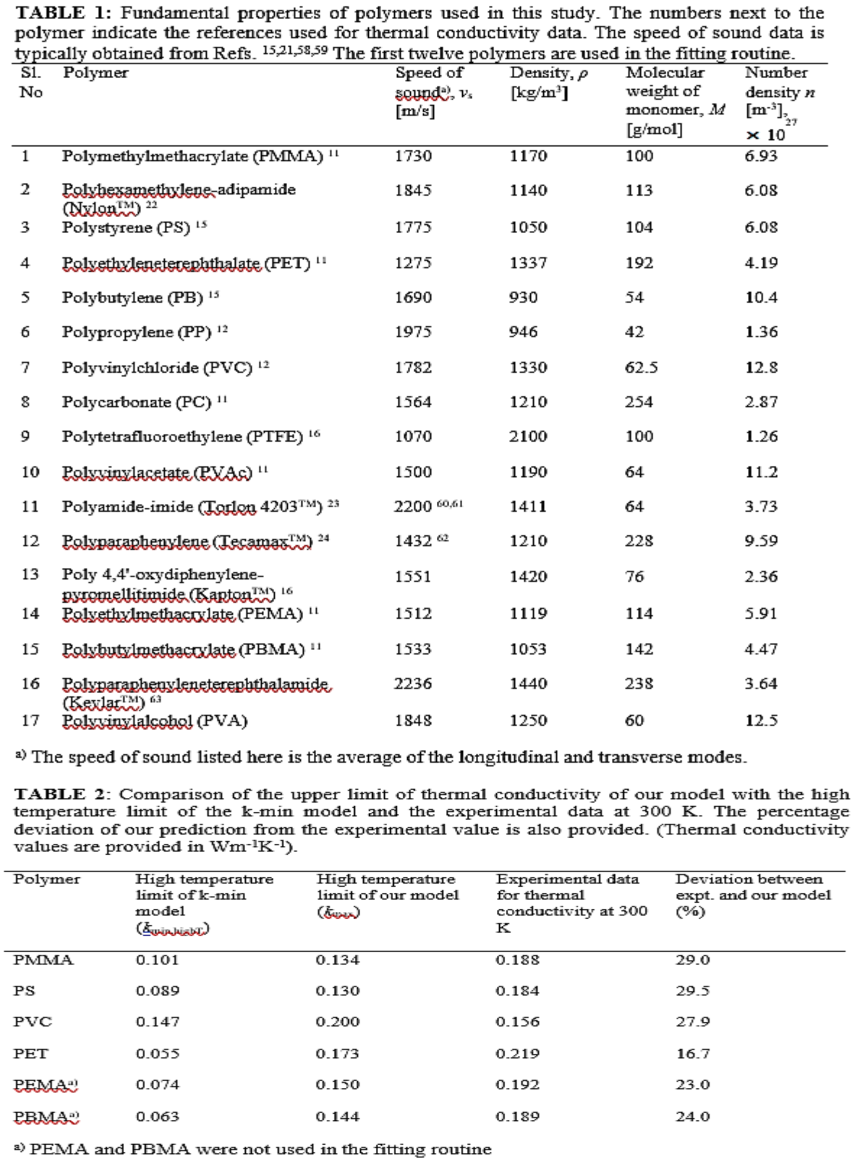

TABLE 1: Fundamental properties of polymers used in this study. The numbers next to the polymer indicate the references used for thermal conductivity data. The speed of sound data is typically obtained from Refs. [15,21,58,59] The first twelve polymers are used in the fitting routine.

Sl. No	Polymer	Speed of sound$^{a)}$, v_s [m/s]	Density, ρ [kg/m^3]	Molecular weight of monomer, M [g/mol]	Number density n [m^{-3}], $\times 10^{27}$
1	Polymethylmethacrylate (PMMA) [11]	1730	1170	100	6.93
2	Polyhexamethylene-adipamide (Nylon™) [22]	1845	1140	113	6.08
3	Polystyrene (PS) [15]	1775	1050	104	6.08
4	Polyethyleneterephthalate (PET) [11]	1275	1337	192	4.19
5	Polybutylene (PB) [15]	1690	930	54	10.4
6	Polypropylene (PP) [12]	1975	946	42	1.36
7	Polyvinylchloride (PVC) [12]	1782	1330	62.5	12.8
8	Polycarbonate (PC) [11]	1564	1210	254	2.87
9	Polytetrafluoroethylene (PTFE) [16]	1070	2100	100	1.26
10	Polyvinylacetate (PVAc) [11]	1500	1190	64	11.2
11	Polyamide-imide (Torlon 4203™) [23]	2200 [60,61]	1411	64	3.73
12	Polyparaphenylene (Tecamax™) [24]	1432 [62]	1210	228	9.59
13	Poly 4,4'-oxydiphenylene-pyromellitimide (Kapton™) [16]	1551	1420	76	2.36
14	Polyethylmethacrylate (PEMA) [11]	1512	1119	114	5.91
15	Polybutylmethacrylate (PBMA) [11]	1533	1053	142	4.47
16	Polyparaphenyleneterephthalamide (Kevlar™) [63]	2236	1440	238	3.64
17	Polyvinylalcohol (PVA)	1848	1250	60	12.5

a) The speed of sound listed here is the average of the longitudinal and transverse modes.

TABLE 2: Comparison of the upper limit of thermal conductivity of our model with the high temperature limit of the k-min model and the experimental data at 300 K. The percentage deviation of our prediction from the experimental value is also provided. (Thermal conductivity values are provided in Wm^{-1}K^{-1}).

Polymer	High temperature limit of k-min model ($k_{min,highT}$)	High temperature limit of our model (k_{max})	Experimental data for thermal conductivity at 300 K	Deviation between expt. and our model (%)
PMMA	0.101	0.134	0.188	29.0
PS	0.089	0.130	0.184	29.5
PVC	0.147	0.200	0.156	27.9
PET	0.055	0.173	0.219	16.7
PEMA$^{a)}$	0.074	0.150	0.192	23.0
PBMA$^{a)}$	0.063	0.144	0.189	24.0

a) PEMA and PBMA were not used in the fitting routine

***Department of Physics**
B.B.D. Govt. College
Chimanpura, Shahpura, Jaipur (Raj.)

References:

1. Snyder, G. J.; Toberer, E. S. Nat Mater 2008, 7, 105-114.
2. He, M.; Qiu, F.; Lin, Z. Energy & Environmental Science 2013, 6, 1352-1361.
3. Zhang, Q.; Sun, Y.; Xu, W.; Zhu, D. Advanced Materials 2014, 26, 6829-6851.
4. Menon, A. K.; Uzunlar, E.; Wolfe, R. M. W.; Reynolds, J. R.; Marder, S. R.; Yee, S. K. Journal of Applied Polymer Science 2017, 134.
5. He, Y.; Donadio, D.; Galli, G. Applied Physics Letters 2011, 98, 144101.
6. Toberer, E. S.; Baranowski, L. L.; Dames, C. Annual Review of Materials Research 2012, 42, 179-209.
7. Cahill, D. G.; Watson, S. K.; Pohl, R. O. Physical Review B 1992, 46, 6131-6140.
8. Kim, J. H.; Feldman, A.; Novotny, D. Journal of Applied Physics 1999, 86, 3959-3963.
9. Russ, B.; Glaudell, A.; Urban, J. J.; Chabinyc, M. L.; Segalman, R. A. Nature Reviews Materials 2016, 1, 16050.
10. Xie, X.; Li, D.; Tsai, T.-H.; Liu, J.; Braun, P. V.; Cahill, D. G. Macromolecules 2016, 49, 972-978.